镀锌钢板电阻点焊涂层电极与普通电极寿命分析

邹家生，　王　涛，　沈　乔，　陈　铮
（江苏科技大学 先进焊接技术省级重点实验室，镇江　212003）

邹家生

摘　要：为增加镀锌钢板电阻点焊电极寿命，在普通铬锆铜电极表面沉积镍和金属陶瓷涂层后，研究涂层电极与无涂层普通电极的寿命. 结果表明，相同条件下，涂层电极使用寿命大约是普通电极使用寿命的 2.5 倍；涂层电极抗塑性变形能力明显高于普通电极；普通电极端面有明显坑蚀、裂纹、合金层、自愈合层，而电极表面涂层能有效防止镀锌钢板电阻点焊过程中由于锌的扩散导致的粘连、剥离，从而减少合金元素 Zn 向电极端面的扩散，防止锌和电极合金形成脆性金属间化合物.

关键词：镀锌钢板；电阻点焊；涂层电极；金属陶瓷涂层；电极寿命
中图分类号：TG115.28　　**文献标识码**：A　　**文章编号**：0253－360X(2011)11－0053－04

0　序　　言

镀锌钢板具有优异防腐特性，近年来在汽车、家电等领域应用越来越广泛. 普通铬锆铜电极在电阻焊镀锌钢板时，熔化锌层粘附于电极端部，与铜合金电极发生合金化，形成硬而脆黄铜层，容易导致电极失效[1,2]. 为了提高电阻焊时电极材料的使用寿命，近年来各国焊接工作者和材料科学家就镀锌钢板电阻焊电极材料进行了大量研究. 通过在电极表面沉积涂层，避免合金化或者减慢合金化. 涂层电极是该领域目前国内外的研究热点之一，其良好的工艺性能、低廉的价格，吸引众多企业和高校积极投入涂层电极研究之中[3,4].

在普通铬锆铜电极表面电火花沉积镍和金属陶瓷复合涂层后，研究对比涂层电极与普通电极的寿命，探讨电极失效机理，为进一步提高镀锌钢板电阻点焊电极寿命提供试验和理论依据.

1　试验方法

1.1　试验材料和设备

采用普通电极为普通锥形铬锆铜电极，涂层电极为在普通电极表面电火花沉积镍和金属陶瓷涂层，具体工艺见文献[5]. 电阻点焊试验采用厚度为 0.7 mm 双面热镀锌钢板，电阻点焊试样尺寸如图 1 所示，采用 S0432NT-8A 交流电阻点焊机进行点焊.

收稿日期：2010－08－23
基金项目：江苏省高技术资助项目(BG2007032)

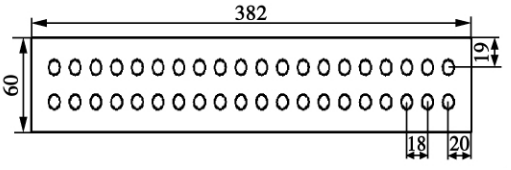

图 1　电阻点焊试样(mm)
Fig. 1　Specimen of resistant spot welding

1.2　点焊电极端面压痕形貌记录

分别采用涂层电极与普通电极对镀锌钢板连续进行点焊，点焊过程中记录第一个点和以后每 100 个焊点电极端面压痕形貌，方法是在镀锌钢板上、下表面均覆盖两张白纸，在两张白纸间夹上一张复写纸. 在两电极臂不通电的条件下，把记录装置放在两电极之间加压一次，则记录装置记录下该对电极第一个点和以后每 100 个焊点端面形貌，同时标上每个记录点的点数[6].

1.3　点焊电极寿命试验

根据美国焊接协会标准 AWS/SAED8.9M:2002，当点焊接头的剪切力第一次小于第 100 个焊点的 80% 时，所对应焊点数的前一点焊点数即为电极寿命. 点焊接头剪切试样如图 2 所示. 试验在 CMT5505 拉伸试验机上进行，夹头位移速率为 10 mm/min[7]. 试验中每 100 个焊点点焊到第 98 个焊点时，将第 99，100，101 这 3 个焊点点焊在剪切试样上，并测定剪切力大小，取其平均值作为每第 100 个焊点的剪切力.

1.4　点焊电极微观分析

当点焊到第300个焊点时，采用JEOL-6480扫

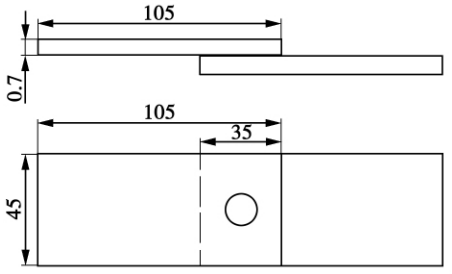

图 2 电阻点焊接头剪切试样(mm)
Fig. 2 Shear specimen of resistant spot welding joints

描电镜(SEM) 对点焊电极进行表面微观形貌分析. 对失效后的电极采用同样的方法进行分析,并和点焊到第 300 焊点的电极进行对比.

2 试验结果及分析

2.1 涂层电极与普通电极端面压痕形貌

不同焊点数下普通电极和涂层电极上、下端面压痕形貌如表 1 所示. 分析表 1 结果可知,起始时普通电极端面压痕粗化明显比涂层电极快,随焊点数增加,粗化倾向趋于一致. 而且上下电极的变化倾向差不多. 说明涂层电极在点焊过程中抵抗初始塑性变形的能力明显强于普通电极.

表 1 电极端面压痕形貌
Table 1 Indentation morphology changes of electrode tip

焊点数	普通电极		涂层电极	
	上电极	下电极	上电极	下电极
0				
100				
300				
500				
800				
1200				
1500				
1800				

从表 1 中发现无涂层电极端面的空白面积明显多于涂层电极. 端面压痕的空白面积是电极端面由于粘连导致剥离而形成的; 这说明电极表面涂层能有效防止镀锌钢板电阻点焊过程中由于扩散导致的粘连、剥离,而且上电极表面的剥离程度要大. 由于电极端面的剥离,必将导致焊点力学性能下降.

仔细观察电极失效后的端面,发现其失效后端面的破坏程度反而比其在焊接过程中的破坏程度要小. 这是由于电极在焊接过程中,电极端面在高温高压的条件下,电极端面不断与自身或与镀锌钢板表面进行微焊接过程,即产生了“自愈合”现象[8].

2.2 涂层电极与普通电极的寿命

普通电极和涂层电极焊接点数对焊点剪切力大小的影响如图 3 和图 4 所示. 从图 3 和图 4 的试验结果可以发现,普通电极点焊接头的剪切力在第 400 个焊点之前基本保持在同一水平位置,大约在 5.9 kN 左右. 从第 500 个焊点开始,普通电极点焊接头剪切力大小逐渐下降,从第 700 个焊点开始急剧下降. 而涂层电极点焊接头剪切力总体变化较小,直到 1 800 个焊点开始才出现急剧下降. 根据美

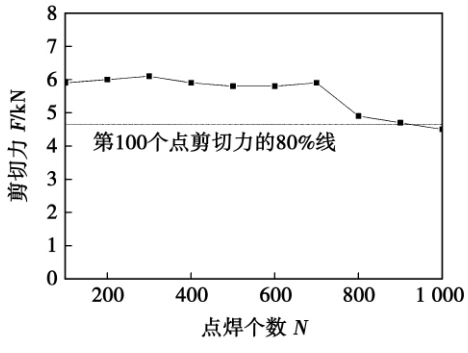

图 3 普通电极焊接点数对焊点剪切力的影响
Fig. 3 Effect of spot-welding number of uncoated electrode on shear strength of joint

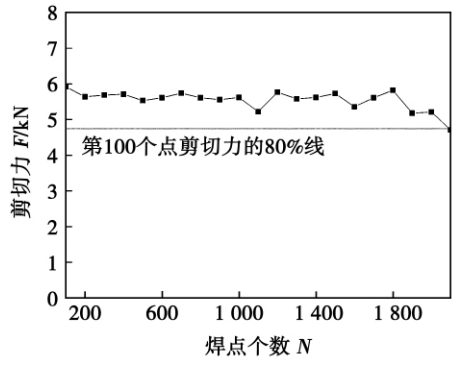

图 4 涂层电极焊接点数对焊点剪切力的影响
Fig. 4 Effect of spot-welding number of coated electrode on shear strength of joint

国焊接协会 AWS 标准，可以得出，点焊普通电极寿命不低于 800 个点，而涂层电极的寿命不低于 2 100 个焊点，故相同条件下，涂层电极的寿命比普通电极提高 2.5 倍以上.

2.3　涂层电极与普通电极端面形貌分析

普通电极和涂层电极第 300 个焊点时的端面宏观形貌如图 5 所示. 普通电极端面覆盖大量银白色物质，而涂层电极表面覆盖的银白色物质面积要少得多.

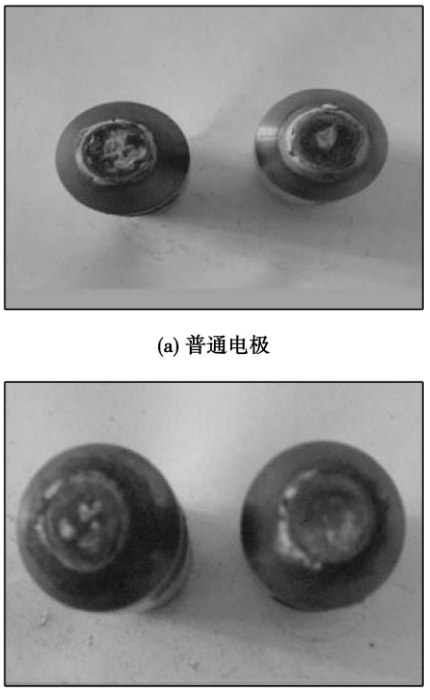

(a) 普通电极

(b) 涂层电极

图 5　普通电极和涂层电极第 300 个焊点时的端面形貌

Fig. 5　Appearance of uncoated and coated electrode at 300th points

普通电极和涂层电极第 300 个焊点时的端面微观形貌如图 6 所示. 由图 6 中可知，普通电极端面粘连的锌层明显多于涂层电极，普通电极端面凹坑明显、损坏严重，而涂层电极端面光滑平整、损坏很小. 所以，在第 300 个焊点时，涂层电极在焊接过程中所受到的损坏程度要比普通电极小得多.

普通电极和涂层电极失效后的宏观和微观形貌如图 7 和图 8 所示. 可以发现普通电极表面粘连了多层金属，存在自愈合沟痕，相比第 300 个焊点时的电极表面，反而变得比较平整. 这主要是普通电极在点焊过程中，受到高温高压的作用，把坑蚀和裂纹进行了多次的微焊接，即“自愈合”现象，同时也包含了电极端面金属因多次挤压导致的塑性变形，使得白色物质已经均匀分布于电极端面. 而失效后的涂层电极端面反而出现不平整现象，出现了凹坑，这

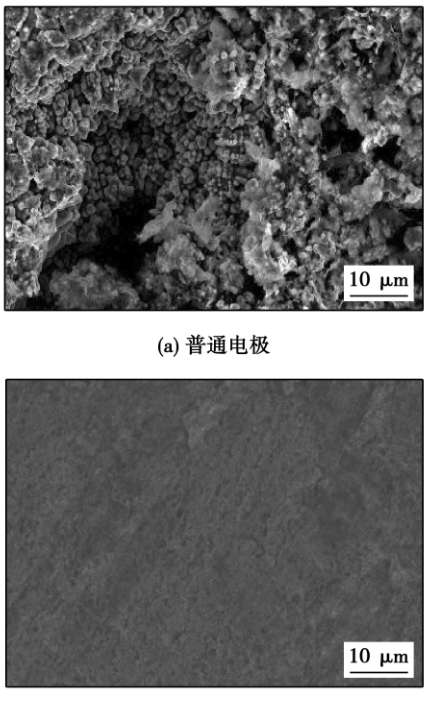

(a) 普通电极

(b) 涂层电极

图 6　普通电极与涂层电极第 300 个焊点时端面微观形貌

Fig. 6　Morphology of uncoated and coated electrode at 300th points

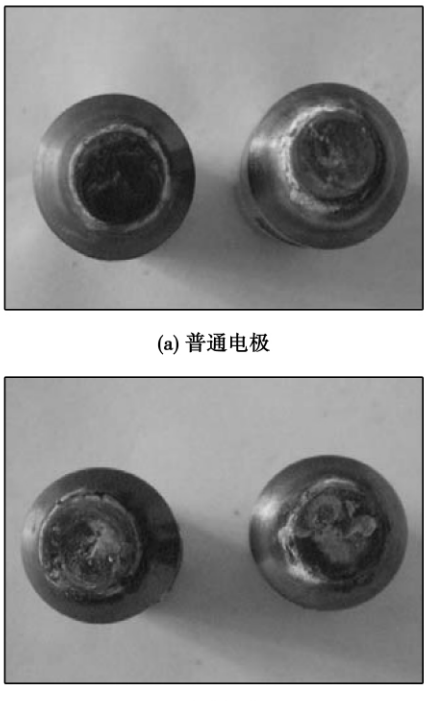

(a) 普通电极

(b) 涂层电极

图 7　普通电极和涂层电极失效后端面宏观形貌

Fig. 7　Appearance of uncoated and coated electrodes after failure

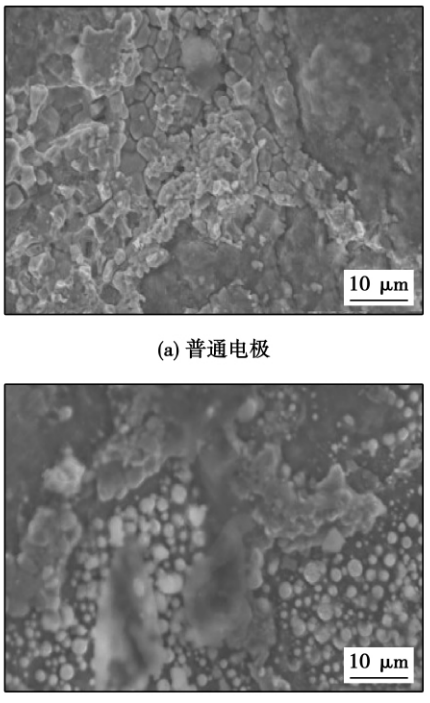

(a) 普通电极

(b) 涂层电极

图 8 失效后普通电极和涂层电极微观形貌

Fig. 8 Morphology of uncoated and coated electrode after failure

种现象与普通电极在第 300 个焊点时的电极端面十分相似,但凹坑深度要小于普通电极在第 300 个焊点时端面凹坑深度,失效后涂层电极表面覆盖有不均匀的白色物,这种白色物很可能是铜镍锌合金和锌层. 这是因为涂层保护着电极端部,阻隔了镀锌钢板镀锌层进入到电极表面,避免了锌层与铬锆铜电极表面发生冶金反应形成铜锌脆性相.

3 结 论

(1) 镀锌钢板电阻点焊时,普通电极端面压痕粗化明显比涂层电极快,涂层电极抗塑性变形能力明显高于普通电极,同时,电极表面涂层能有效防止镀锌钢板电阻点焊过程中由于锌的扩散导致的粘连、剥离.

(2) 普通电极端面有明显坑蚀、裂纹、合金层、自愈合层,而相同条件下,涂层电极在焊接过程中所受到的损坏程度要比普通电极小得多.

(3) 在相同试验条件下,电阻点焊接头剪切力标准测定电极寿命的试验结果得出,普通电极的使用寿命不少于 800 次,而涂层电极的使用寿命不少于 2 100 次,相比无涂层电极,涂层电极的使用寿命提高了约 2.5 倍.

(4) 电极表面涂层作为一个屏障能显著减少合金元素 Zn 向电极端面的扩散,从而有效防止锌和电极合金形成脆性金属间化合物.

参考文献:

[1] 陈艳青. 制备镀锌钢板电阻焊涂层电极电火花沉积技术的研究[D]. 镇江: 江苏科技大学, 2009.

[2] Zou Jiasheng, Zhao Qizhang, Chen Zheng. Surface modified long-life electrode for resistance spot welding[J]. Journal of Materials Processing Technology, 2009, 209(8): 4141 - 4146.

[3] 程长坤. 提高电阻点焊镀锌钢板电极寿命的方法及展望[J]. 湖北汽车工业学院报, 2005, 5(6): 23 - 24.
Cheng Changkun. Method and prospect of improving the life of resistance spot welding electrodes[J]. Hubei Institute of Automobile Industry Report, 2005, 5(6): 23 - 24.

[4] 殷美庆, 王 敏, 蒋镜昱, 等. 镀锌钢板点焊电极寿命研究[J]. 电焊机, 2003, 33(5): 14 - 17.
Yin Meiqing, Wang Min, Jiang Jingyu, *et al*. Research of electrode life in spot welding of galvanized steel sheet[J]. Welding Machine, 2003, 33(5): 14 - 17.

[5] 沈 乔. 镀锌钢板电阻点焊涂层电极研究[D]. 镇江: 江苏科技大学硕士论文, 2010.

[6] 程长坤. 点焊电极表面能振动电火花熔敷 TiC 的研究[D]. 武汉: 武汉科技大学, 2004.

[7] Levashov E A. Nanopartical dispersion-strengthened coatings and electrode materials for electro-spark deposition[J]. Thin Solid Films, 2006, 515: 1161 - 1165.

[8] Chatterjee K L, Waddell W. Electrode wear during spot welding of coated steel[J]. Welding & Metal Fabrication, 1996(3): 110 - 114.

作者简介: 邹家生,男,1965 年出生,博士,教授. 主要研究方向为新材料及其连接技术. 发表论文 90 余篇. Email: zjzoujs@126.com

tail of the weld pool and the slag are effectively divided in the way mentioned above, which is superior to the segmentation method based on Sobel operator and single fractal dimension algorithm.

Key words: fractal dimension; arc welding; multi-scale fractal; weld seam formation; welding pool image segmentation

Extracting weld seam by Hough transform based on dynamic windows DENG Jingyu, QIN Tao, ZHANG Ke, JIN Xin (Shanghai Key Laboratory of Laser Manufacturing & Material Modification, Shanghai Jiaotong University, Shanghai 200240, China). p 37 - 40

Abstract: Based on the similarity of the former and later image in the seam tracking process and the coordinates of the previous pictures´ three characteristic points, dynamic region of interested can be extracted from the current image. And the range of Hough transform parameter space´s θ parameter is determined by the value of θ_0 parameter of the previous image and then each piece of dynamic image of region of interested is processed by Hough transform. The dynamic window and limiting Hough transform parameter space´s θ range can significantly speed up the search for an effective pixel and reduce the Hough transform calculation. Experiments indicate that this method can greatly increased computational speed and algorithm stability and accuracy of fitted straight line, and meet the requirements of real-time seam tracking.

Key words: Hough transform; dynamic windows seam tracking; line fitting

Hybrid interaction of laser and pulsed MIG arc and its influence on metal transfer WEI Huiliang[1], LI Huan[1], WANG Xuyou[2], WANG Wei[2], GAO Ying[3] (1. Tianjin Key Laboratory of Advanced Joining Technology, Tianjin University, Tianjin 300072, China; 2. Harbin Welding Institute, Harbin 150080, China; 3. Tianjin Key Laboratory of High Speed Cutting and Precision Machining, Tianjin University of Technology and Education, Tianjin 300222, China). p 41 - 44

Abstract: Experiments were conducted to research the mutual effect, the interaction of laser and MIG arc and the influence of the addition of laser on the form of MIG arc and the type of metal transfer. The YAG laser and pulsed MIG hybrid welding system was established. In addition, high-speed photography system was used to observe the arc behavior and metal transfer, with the current signals and voltage signals of the arc collected synchronously. It was found that the metal transfer mode changed from one droplet per pulse to one droplet every two pulses with the addition of laser to MIG welding. Pulsed MIG arc could be apparently attracted by laser. The decrease of the vertical-force component of plasma force which could promote metal transfer was the main reason that caused the decline of the frequency of metal transfer.

Key words: hybrid welding; metal transfer; high-speed photography

Wettability enhancement of Al-Si brazing filler on stainless steel using plasma Al ion implantation WANG Guowei, XU Muzhong, TIAN Xiubo, GONG Chunzhi, YANG Shiqin (State Key Lab of Advanced Welding & Joining, Harbin Institute of Technology, Harbin 150001, China). p 45 - 48

Abstract: MEVVA ion source was used to implant Al directly into stainless steel to improve the wettability of the filler metal. The surface chemical composition of the implanted layer was characterized by X-ray photoelectron spectroscopy (XPS). The wettability of BAl88Si on stainless steels was investigated by metallographic microscope and scanning electron microscope (SEM). Aluminum was observed within the top surface of stainless steel after ion implantation. BAl88Si did not wet on unmodified stainless steel at 600 ℃ and 610 ℃. If the temperature was elevated to 650 ℃, the BAl88Si solder demonstrated some wettability on unmodified stainless steel with the wetting angle of over 40°. Al ion implantation plays an important role on the improvement of wettability. With implantation dose of 9×10^{17} ions/cm^2 and the extraction voltage of 40 kV, BAl88Si exhibits good wettability on implanted samples, even at 600 ℃. A wetting angle of about 20° was achieved and satisfied the brazing demand of aluminum onto stainless steel.

Key words: MEVVA source; ion implantation; BAl88Si; wettability; stainless steel

He and He + CO_2 double shielded TIG welding process QIN Mingpeng, LI Dongjie, LU Shanping (Shenyang National Laboratory for Materials Science, Institute of Metal Research, Chinese Academy of Sciences, Shenyang 110016, China). p 49 - 52

Abstract: He and He + CO_2 double shielded TIG welding process was proposed to study the electrode protection and weld shape variations of 0Cr13Ni5Mo low carbon martensite stainless steel used for hydraulic turbine runners. Pure inert gas(He) as inner layer, avoids the electrode directly contacting the outer layer active gas(CO_2) and being oxidized. Addition CO_2 to the outer layer shielding gas provides a surface active element (oxygen) which dissolves into the weld pool to change the Marangoni convection mode and weld shape. The results show that the electrode is successfully protected, and Marangoni convection changes from outward to inward to produce a deep and narrow weld when the weld oxygen content is between 0.007 6% ~0.012% in weld metal. The double shielded TIG welding is more than twice the welding efficiency of the conventional TIG welding.

Key words: electrode protection; weld shape; oxygen content; marangoni convection

Investigation on life of coated electrode and traditional electrode for resistant spot welding of Zn-coated steels ZOU Jiasheng, WANG Tao, SHEN Qiao, CHEN Zheng (Provincial Key Lab of Advanced Welding Technology, Jiangsu University of Science and Technology, Zhenjiang 212003, China). p 53 - 56

Abstract: A nickel and a metallic ceramic coating were deposited on to the end surface of a traditional Cr-Zr-Cu resistant welding electrode in order to increase the life of electrode for resistant spot welding of Zn-coated sheet steels. The life of the coated electrode was approximately two and half times than that of the uncoated electrode under the same experimental conditions.

The coated electrode had higher ability to prevent the electrode from plastic deformation during welding compared with the un-coated electrode. In addition, there were much more pitting, cracking, intermetallic alloy layer and self-healing layer on the end surface of un-coated electrode. As a barrier, the coatings on the surface of electrode could effectively prevent the adhesions, stripping, and then significantly reduce the diffusion of Zn from the surface of the electrode into the Cr-Zr-Cu electrode to form brittle intermetallic compounds.

Key words: Zn-coated sheet steel; resistant spot welding; coated electrode; metallic ceramic coating; electrode life

Control system for electron beam synchronous scanning based on CPLD PENG Yong[1], WANG Kehong[1], ZHOU Qi[1], WANG Yajun[2], FU Pengfei[3] (1. School of Materials Science and Engineering, Nanjing University of Science and Technology, Nanjing 210094, China; 2. School of Mechanical Engineering and Automation, Beijing University of Aeronautics and Astronautics, Beijing 100083, China; 3. National Key Laboratory of High Power Beam Processing Technology, Beijing Aeronautical Manufacturing Technology Research Institute, Beijing 100024, China). p 57 - 60

Abstract: For the quality diagnosis of electron beam in range from 5 mA to 60 mA of a high-voltage electron beam welding machine, a CPLD (Complex Programmable Logic Device) -based control system of electron beam high-speed scanning was established by means of analyzing the principle of electron beam scanning in the electromagnetic deflection coils. The control system consists of industrial PC, CPLD chip, DAC (Digital to Analog Convertor), low pass filter circuits, optical isolation circuits, power amplifiers, electromagnetic deflection coil and external circuits of CPLD. The system controls the special phase relationship between the two waveform and the trigger and sampling frequency of the acquisition card. The scanning frequency can be adjusted within the range 0 ~ 15.6 kHz. The amplified power is the constant current mode and its maximum output current is 5 A. The signal parameters can be adjusted to change the scanning path of electron beam without changing any hardware circuit, so it is highly flexible.

Key words: electron beam welding; CPLD; synchronous scanning; beam quality

Friction-stir welds (FSW) of spray formed 7475 aluminum alloy plate YAN Keng, SHI Chao (Provincial Key Lab of Advanced Welding Technology, Jiangsu University of Science and Technology, Zhenjiang 212003, China). p 61 - 64

Abstract: Friction-stir welds (FSW) of spray formed 7475 aluminum alloy plate with 4 mm thickness were studied. The shapes and dimensions of FSW tools as well as welding parameters were optimized based on mechanical tests and micro-analysis. Experimental results show that good-appearance welds can be achieved by optimal welding parameters. However, fin and groove defects appear if the welding parameters are not appropriate. It also shows that the mechanical properties of the joints are affected by the welding parameters. Some relations between the mechanical properties and the welding parameters were established. As the rotating speed is 1 200 r/min and the welding speed is 80 mm/min, the good weld is achieved and the tensile strength of the weld reaches 442 MPa.

Key words: spray formed 7475 aluminum alloy; FSW; technique; mechanical property

Influence of Ni on microstructure and processing performance of Ag-Cu-Sn-In brazing alloy XU Jinfeng[1], ZHANG Xiaocun[1], ZHAI Qiuya[1], DAI Weigang[2] (1. School of Materials Science and Engineering, Xi'an University of Technology, Xi'an 710048, China; 2. Changshu Shuanghua Electronic Co., Ltd., Changshu 215500, China). p 65 - 68

Abstract: Influence of Ni on the microstructure and processing performance of Ag-Cu-Sn-In brazing alloy was investigated. The microstructures of Ag-Cu-Sn-In of solder were composed of β-Cu coarse dendrite, (α-Ag) distributing in the interdendritic space and little Ag_5Sn. By adding Ni element, the grains refined, the melting point rised a little, and processability was influenced evidently. With Ni content increasing, rate of deformation is bigger, processability of brazing alloy is better. As Ni content was 0.2%, the rate of deformation reached maxinum. Ni content sequentially increasing, microstructures of brazing alloy are becoming bulkily, and processability is worse. With 0.2% Ni Content, the temperature of solidus and liquidus of alloy foils increased respectively by 18 ℃ and 8 ℃, the temperature interval decreased by 20 ℃. After annealing treatment, brazing alloy with 0.2% Ni can be rolled into foils of 50 ~ 80 μm thickness.

Key words: lower silver electrical vacuum brazing filler; melting point; microstructure; processability

Wettability and microstructure of Sn-Ag-Cu-In solder WANG Jianxin, YIN Ming, LAI Zhongmin, LI Xue (Province Key Lab of Advanced Welding Technology, Jiangsu University of Science and Technology, Zhenjiang 212003, China). p 69 - 72

Abstract: In order to improve the properties of Sn-1.2Ag-0.6Cu solder, small amount of In (0 ~ 1.0%) was added to the base alloys, the melting temperatures of alloys were tested, and the effect of In on the wettability and microstructure of solder alloy was studied. The melting temperature decreases with the addition of In. At the same soldering temperature, the lower melting temperature is, the higher superheat is, thus the viscosity of liquid solder is decreased and fluidity is improved. The zero time of Sn-1.2Ag-0.6Cu in air is below 1s at 260℃, while the zero time of Sn-1.2Ag-0.6Cu-1.0In in N_2 atomsphere is below 1s at 250℃, meeting the demand of IPC/EIA J-STD-003B. The Ag_3Sn in Sn-1.2Ag-0.6Cu alloy becomes coarser with 1.0% In added, which is harmful to the mechanical properties. Thenefore, the content of In addition into the Sn-1.2Ag-0.6Cu is not higher than 1.0%.

Key words: lead-free solder; wettability; microstructure

SMT soldering image denoising based on wavelet packet transform and adaptive threshold ZHAO Huihuang[1,2], ZHOU Dejian[3], WU Zhaohua[3], LI Chunquan[3], LI Kangman[1] (1. Department of Computer, Hengyang Normal University, HengYang 421008, China; 2. School of Mechano-Electronic Engineering, Xidian University, Xi'an 710071, China; 3. School of Mechanical and Electronical Engineering, Guilin University of